NUMERICAL STUDY OF THE TURBULENT NATURAL CONVECTION OF NANOFLUIDS IN A PARTIALLY HEATED CUBIC CAVITY

by

Zakaria LAFDAILI[a*], Sakina EL-HAMDANI[a], Abdelaziz BENDOU[a], Karim LIMAM[b], and Bara EL-HAFAD[a]

[a] Laboratory for Mechanics, Processes, Energy and Environment (LMPEE), National School of Applied Sciences, University Ibn Zohr, Agadir, Morocco
[b] LASIE, University La Rochelle, La Rochelle Cedex 1, France

Original scientific paper
https://doi.org/10.2298/TSCI200513057L

In this work we study numerically the 3-D turbulent natural convection in a partially heated cubic cavity filled with water containing metallic nanoparticles, metallic oxides, and others based on carbon. The objective is to study and compare the effect of the addition of nanoparticles studied in water and also the effect of the position of the heated partition on the heat exchange by turbulent natural convection in this type of geometry, which can significantly improve the design of heat exchange systems for better space optimization. For this we have treated numerically for different volume fractions the turbulent natural convection in the two cases where the cavity is heated respectively by a vertical and horizontal strip in the middle of one of the vertical walls. To take into account the effects of turbulence, we used the standard k-ε turbulence model. The governing equations are discretized by the finite volume method using the power law scheme which offers a good stability characteristic in this type of flow. The results are presented in the form of isothermal lines and current lines. The variation of the mean Nusselt number is calculated for the two positions of the heated partition as a function of the volume fraction of the nanoparticles studied in water for different Rayleigh numbers. The results show that carbon-based nanoparticles intensify heat exchange by convection better and that the position of the heated partition significantly influences heat exchange by natural convection. In fact, an improvement in the average Nusselt number of more than 20% is observed for the case where the heated partition is horizontal.

Key words: *convection, natural, turbulence, nanofluid, cubic*

Introduction

Today, with the permanent growth in energy prices, its control has become a major challenge in all areas of activity. For energy professionals, the first challenge is to design energy systems and processes with better efficiencies. The increased demand for the performance of these thermal systems has always aroused considerable interest in techniques for improving heat transfer. The technological importance of heat transfer by natural convection is confirmed by its use in different fields such as metallurgy, the food industry, solar technology, cooling of nuclear reactors, cooling of electronic circuits and transformers, *etc.*, it then becomes necessary to properly quantify the heat exchanges between a heated wall and a flow-

* Corresponding author, e-mail: zakaria.lafdaili@edu.uiz.ac.ma

ing fluid for better design and optimal use of heat exchange systems. The thermophysical properties of the heat transfer fluids used often limit the efficiency of such processes. But with advances in nanotechnology, the idea of suspending nanoscale particles in a base liquid has improved its thermal properties for better intensification of heat transfer.

The study of the natural convection of nanofluids in cavities has been the subject of a very large number of works, both theoretical and experimental. Choi and Eastman [1] by dispersing TiO_2 nanoparticles with a diameter of 27 nm in water, obtained an improvement in thermal conductivity of 10.7% for a volume fraction of 4.35%. This value is much lower than the 32% obtained for the nanofluid (water + Al_2O_3) with the same concentration of nanoparticles. Namburu *et al.* [2] presented a monophasic model to study numerically the heat transfer characteristics of a nanofluid in a circular tube where the flow is in turbulent regime. They found that the Nusselt number is greater for the small diameters of nanoparticles. Other researchers have thought of other models. Indeed, [3] and Mirmasoumi and Bezadmehe [4] used the two-phase model of a nanofluid in a tube in forced natural convection.

Much more work has been done over the past decade to characterize nanofluids. Irfan *et al.* [5] analyzed the improvement of heat transfer by natural convection of nanofluids through a vertical corrugated plate subjected to a variable heat flux. They found that the rate of heat transfer in Al_2O_3- and Cu-based nanofluids compared to pure water can be increased due to the increased concentration of nanoparticles. Fallah *et al.* [6] have studied numerically the effect of the volume fraction of Al_2O_3 nanoparticles in water on the hydrodynamic and thermal characteristics in natural convection in a concentric horizontal annular enclosure for Rayleigh numbers ranging from 10^3 to 10^5. Javed *et al.* [7] presented a detailed literature related to studies on heat transfer by natural convection of nanofluids in different flow regimes for different heat transfer devices such as tubes, heat sinks, heat exchangers, *etc.* The authors highlighted the effect of the flow regime, the type of nanofluid used, the size of the nanoparticles, the temperature and the concentration of nanoparticles on the thermal characteristics of the nanofluid.

Other studies have highlighted the effects of the geometrical appearance of confined enclosures, as well as their heating mode on convective heat transfer. Mendu *et al.* [8] studied the natural convection of nanofluids in a square enclosure embedded with a discrete heating element at the bottom to highlight the effect of the position of the heater on the heat exchange. Aghajani *et al.* [9] also studied the effect of the location of the heating resistance on heat transfer and the generation of entropy in a cavity. Their results show that the location of the heater has a significant effect on the flow pattern and temperature fields within the enclosure and, subsequently, on the generation of entropy. Indeed, a greater heat transfer was observed when the heater is located on a vertical wall. Terekhova *et al.* [10] studied the influence of the geometry of the enclosure on the 3-D flow structure and heat transfer. They have shown that the 3-D nature of the flow has a profound effect on heat transmission for smaller form ratios (F.R <1). For longer enclosures, the heat emission coefficient is not entirely related to the height/width ratio of the enclosure and can be determined by a 2-D approach.

The turbulent nature can also considerably influence convective flows by improving mixtures and heat and mass transfers [11-13]. Knowledge of these phenomena can therefore contribute to the development of strategies for controlling or optimizing heat and mass transfers or transport.

Most studies of natural convection have dealt with 2-D configurations. To get closer to reality and constitute a research fund for heat exchange systems, we study numerically the flow of nanofluids in a 3-D cavity (cube) in order to highlight the effects of the volume fraction, Φ, of the nanoparticles studied in water and the effect of the position of the heating strip in the vertical wall on the turbulent natural convection.

Modeling and equations

The configuration studied is shown in fig. 1 is a cubic cavity, filled with water containing different concentrations of nanoparticles. The cavity is formed by a vertical wall containing in its center a vertical/horizontal band representing 25% of its surface and maintained at a hot temperature, T_h, a straight vertical wall maintained at a constant cold temperature, T_c and two other horizontal walls considered adiabatic.

All the thermophysical properties of nanofluids are considered constant, except for the variation of the density which is estimated by the Boussinesq approximation. Table 1 groups together in the thermophysical properties of the pure fluid and of the nanoparticles studied.

Table 1. Thermophysical properties of water and nanoparticles

	Pr	ρ [kgm^{-3}]	Cp [Jkg^{-1}K^{-1}]	k [Wm^{-1}K^{-1}]	β [10^{-5} K^{-5}]<<<<<<<<<<<<(10^{-5}K^{-1}(10^{-5}K^{-1}	Reference
Pure water	4.7	997	4179	0.613	21	[13]
Al_2O_3	–	3970	765	40	0.85	[13]
CuO	–	6500	540	18	1.0	[14]
Cu_2O	–	6080	474	42	0.19	[15]
Fe_3O_4	–	5200	670	6	1.3	[16]
MgO		3580	879	45	3.36	[17]
SiO_2	–	3970	765	36	0.63	[18]
TiO_2	–	4250	686.2	8.95	0.9	[19]
ZnO	–	5600	495	80	3	[20]
ZrO_2	–	5600	418	2.6	0 .85	[21]
Au	–	19300	129	318	1.42	[22]
Ag	–	10500	235	429	1.89	[22]
Cu	–	8933	385	400	1.67	[22]
Co	–	8900	420	100	1.2	[23]
MoS_2	–	5060	397.21	904.4	2.34	[24]
Nimonic 80A	–	8190	448	112	1.27	[25]
SiC	–	3160	675	490	0.3	[26]
Steel	–	8030	502.48	16.27	1.2	[27]
C60	–	3500	509	2300	1.72	[26]
Diamond	–	3510	497.26	1000	0.1	[28]
GO	–	1800	717	5000	28.4	[19]
MWCNT	–	1600	796	3000	0 .1	[29]
SWCNT	–	2600	425	6600	0 .1	[29]

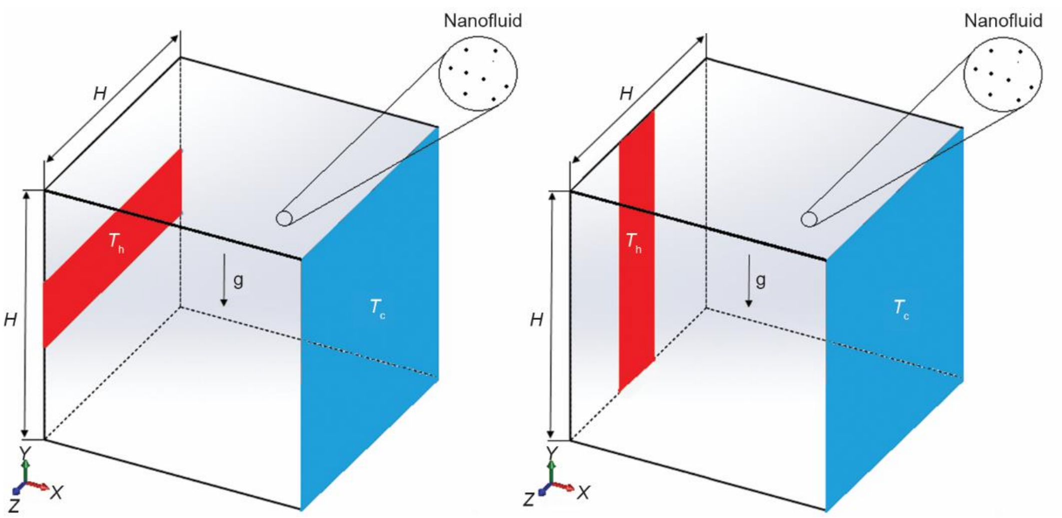

Figure 1. Geometry and limit conditions of the configuration studied

To account for the effects of turbulence, the *k*-*ε* model is used. Therefore, the governing equations written in the Cartesian co-ordinate system (*x*, *y*, *z*) are:

– equation of continuity

$$\frac{\partial(\rho u)}{\partial x}+\frac{\partial(\rho v)}{\partial y}+\frac{\partial(\rho w)}{\partial z}=0 \tag{1}$$

– momentum equation in the *x*-direction

$$\rho_{\mathrm{nf}}u\frac{\partial u}{\partial x}+\rho_{\mathrm{nf}}v\frac{\partial u}{\partial y}+\rho_{\mathrm{nf}}w\frac{\partial u}{\partial z}=-\frac{\partial p}{\partial x}+\frac{\partial}{\partial x}\left\{[\mu_{\mathrm{nf}}+(\mu_{\mathrm{t}})_{\mathrm{nf}}]\left(2\frac{\partial u}{\partial x}\right)\right\}+$$
$$+\frac{\partial}{\partial y}\left\{[\mu_{\mathrm{nf}}+(\mu_{\mathrm{t}})_{\mathrm{nf}}]\times\left(\frac{\partial u}{\partial y}+\frac{\partial v}{\partial x}\right)\right\}+\frac{\partial}{\partial z}\left\{[\mu_{\mathrm{nf}}+(\mu_{\mathrm{t}})_{\mathrm{nf}}]\left(\frac{\partial u}{\partial z}+\frac{\partial w}{\partial x}\right)\right\} \tag{2}$$

– momentum equation in the *y*-direction

$$\rho_{\mathrm{nf}}u\frac{\partial v}{\partial x}+\rho_{\mathrm{nf}}v\frac{\partial v}{\partial y}+\rho_{\mathrm{nf}}w\frac{\partial v}{\partial z}=-\frac{\partial p}{\partial y}+\frac{\partial}{\partial y}\left\{[\mu_{\mathrm{nf}}+(\mu_{\mathrm{t}})_{\mathrm{nf}}]\left(2\frac{\partial v}{\partial y}\right)\right\}+$$
$$+\frac{\partial}{\partial x}\left\{[\mu_{\mathrm{nf}}+(\mu_{\mathrm{t}})_{\mathrm{nf}}]\times\left(\frac{\partial u}{\partial y}+\frac{\partial v}{\partial x}\right)\right\}+\frac{\partial}{\partial z}\left\{[\mu_{\mathrm{nf}}+(\mu_{\mathrm{t}})_{\mathrm{nf}}]\left(\frac{\partial w}{\partial y}+\frac{\partial v}{\partial z}\right)\right\}+\mathrm{g}\rho_{\mathrm{nf}}\beta_{\mathrm{nf}}(T-T_{\mathrm{ref}}) \tag{3}$$

– momentum equation in the *z*-direction

$$\rho_{\mathrm{nf}}u\frac{\partial w}{\partial x}+\rho_{\mathrm{nf}}v\frac{\partial w}{\partial y}+\rho_{\mathrm{nf}}w\frac{\partial w}{\partial z}=-\frac{\partial p}{\partial z}+\frac{\partial}{\partial z}\left\{[\mu_{\mathrm{nf}}+(\mu_{\mathrm{t}})_{\mathrm{nf}}]\left(2\frac{\partial w}{\partial z}\right)\right\}+$$
$$+\frac{\partial}{\partial x}\left\{[\mu_{\mathrm{nf}}+(\mu_{\mathrm{t}})_{\mathrm{nf}}]\times\left(\frac{\partial u}{\partial y}+\frac{\partial v}{\partial x}\right)\right\}+\frac{\partial}{\partial y}\left\{[\mu_{\mathrm{nf}}+(\mu_{\mathrm{t}})_{\mathrm{nf}}]\left(\frac{\partial v}{\partial z}+\frac{\partial w}{\partial y}\right)\right\} \tag{4}$$

– thermal energy equation

$$\rho_{\rm nf} u\frac{\partial T}{\partial x}+\rho_{\rm nf} v\frac{\partial T}{\partial y}+\rho_{\rm nf} w\frac{\partial T}{\partial z}=\frac{\partial}{\partial x}\left\{\left[\frac{\mu_{\rm nf}}{\mathrm{Pr}_{\rm nf}}+\frac{(\mu_t)_{\rm nf}}{\sigma_{\rm t}}\right]\frac{\partial T}{\partial x}\right\}+$$
$$+\frac{\partial}{\partial y}\left\{\left[\frac{\mu_{\rm nf}}{\mathrm{Pr}_{\rm nf}}+\frac{(\mu_t)_{\rm nf}}{\sigma_{\rm t}}\right]\frac{\partial T}{\partial y}\right\}+\frac{\partial}{\partial z}\left\{\left[\frac{\mu_{\rm nf}}{\mathrm{Pr}_{\rm nf}}+\frac{(\mu_t)_{\rm nf}}{\sigma_{\rm t}}\right]\frac{\partial T}{\partial z}\right\} \tag{5}$$

– turbulent kinetic energy equation

$$\rho_{\rm nf} u\frac{\partial k}{\partial x}+\rho_{\rm nf} v\frac{\partial k}{\partial y}+\rho_{\rm nf} w\frac{\partial k}{\partial z}=\frac{\partial}{\partial x}\left\{\left[\mu_{\rm nf}+\frac{(\mu_t)_{\rm nf}}{\sigma_k}\right]\frac{\partial k}{\partial x}\right\}+$$
$$+\frac{\partial}{\partial y}\left\{\left[\mu_{\rm nf}+\frac{(\mu_t)_{\rm nf}}{\sigma_k}\right]\frac{\partial k}{\partial y}\right\}+\frac{\partial}{\partial z}\left\{\left[\mu_{\rm nf}+\frac{(\mu_t)_{\rm nf}}{\sigma_k}\right]\frac{\partial k}{\partial z}\right\}+(P_k)_{\rm nf}+(G_k)_{\rm nf}-\rho_{\rm nf}\varepsilon \tag{6}$$

– equation for the rate of energy dissipation

$$\rho_{\rm nf} u\frac{\partial \varepsilon}{\partial x}+\rho_{\rm nf} v\frac{\partial \varepsilon}{\partial y}+\rho_{\rm nf} w\frac{\partial \varepsilon}{\partial z}=\frac{\partial}{\partial x}\left\{\left[\mu_{\rm nf}+\frac{(\mu_t)_{\rm nf}}{\sigma_\varepsilon}\right]\frac{\partial \varepsilon}{\partial x}\right\}+\frac{\partial}{\partial y}\left\{\left[\mu_{\rm nf}+\frac{(\mu_t)_{\rm nf}}{\sigma_\varepsilon}\right]\frac{\partial \varepsilon}{\partial y}\right\}+$$
$$+\frac{\partial}{\partial z}\left\{\left[\mu_{\rm nf}+\frac{(\mu_t)_{\rm nf}}{\sigma_\varepsilon}\right]\frac{\partial \varepsilon}{\partial z}\right\}+\left\{C_{\varepsilon 1} f_1[(P_k)_{\rm nf}+C_{\varepsilon 3}(G_k)_{\rm nf}]-\rho_{\rm nf} C_{\varepsilon 2} f_2\varepsilon\right\}\frac{\varepsilon}{k} \tag{7}$$

The $(P_k)_{\rm nf}$ represents the stress production and is calculated:

$$(P_k)_{\rm nf}=(\mu_t)_{\rm nf}\left[2\left(\frac{\partial u}{\partial x}\right)^2+2\left(\frac{\partial v}{\partial y}\right)^2+2\left(\frac{\partial w}{\partial z}\right)^2+\left(\frac{\partial u}{\partial y}+\frac{\partial v}{\partial x}+\frac{\partial w}{\partial z}\right)^2\right] \tag{8}$$

The $(G_k)_{\rm nf}$ is the buoyancy term, and is defined:

$$(G_k)_{\rm nf}=\frac{(\mu_t)_{\rm nf}}{\sigma_t}\mathrm{g}\beta_{\rm nf}\frac{\partial T}{\partial y} \tag{9}$$

The Prandtl number is calculated:

$$\mathrm{Pr}_{\rm nf}=\frac{Cp_{\rm nf}\,\mu_{\rm nf}\,K_{\rm eff,f}}{Cp_{\rm f}\,\mu_{\rm f}\,K_{\rm eff,nf}}\mathrm{Pr} \tag{10}$$

The following formulas were used to compute the thermal and physical properties of the nanofluids under consideration.

The eddy viscosity is calculated:

$$(\mu_t)_{\rm nf}=\rho_{\rm nf} C_\mu f_\mu\frac{k^2}{\varepsilon} \tag{11}$$

The dynamic viscosity of the nanofluid defined by the Brinkman model [30]:

$$\mu_{\mathrm{nf}} = \frac{\mu_f}{(1-\Phi_{\mathrm{p}})^{2.5}} \tag{12}$$

The $K_{\mathrm{eff,nf}}$, the effective thermal conductivity of the nanofluid defined by the Maxwell-Garnetts model [31]:

$$K_{\mathrm{eff,nf}} = K_{\mathrm{eff,f}} \left[\frac{(K_{\mathrm{eff,p}} + 2K_{\mathrm{eff,f}}) - 2\Phi(K_{\mathrm{eff,f}} - K_{\mathrm{eff,p}})}{(K_{\mathrm{eff,p}} + 2K_{\mathrm{eff,f}}) + \Phi(K_{\mathrm{eff,f}} - K_{\mathrm{eff,p}})} \right] \tag{13}$$

The equations (13)-(15) are general relationships used to compute the density, the coefficient of thermal expansion and the heat capacity for a classical two-phase mixture [32].

$$\rho_{\mathrm{nf}} = (1-\Phi)\rho_{\mathrm{f}} + \Phi\rho_{\mathrm{p}} \tag{14}$$

$$\beta_{\mathrm{nf}} = (1-\Phi)\beta_{\mathrm{f}} + \Phi\beta_{\mathrm{p}} \tag{15}$$

$$Cp_{\mathrm{nf}} = (1-\Phi)Cp_{\mathrm{f}} + \Phi Cp_{\mathrm{p}} \tag{16}$$

The empirical constants were recommended by Launder and Spalding [33] is listed in tab. 2.

Table 2. The values of the constants in the *k-ε* model

C_μ	$C_{\varepsilon 1}$	$C_{\varepsilon 2}$	σ_k	σ_ε
0.09	1.44	1.92	1.0	1.33

By analogy with the expression of $C_{\varepsilon 3}$ suggested by Henkes [34], we use the following expression:

$$C_{\varepsilon 3} = \tanh\left[\frac{\left(\frac{v}{u} + \frac{v}{w} \right)}{2} \right] \tag{17}$$

All physical properties were estimated at the average temperature:

$$T_{\mathrm{ref}} = \frac{T_{\mathrm{h}} + T_{\mathrm{c}}}{2} \tag{18}$$

The average Nusselt number $\mathrm{Nu_{av}}$ of the hot wall is expressed:

$$\mathrm{Nu_{av}} = -\frac{K_{\mathrm{eff,f}}}{H^2 K_{\mathrm{eff,nf}}} \int_0^H \int_0^H \left. \frac{\partial T}{\partial x} \right)_{x=L} \mathrm{d}x \tag{19}$$

The Rayleigh number is defined:

$$\mathrm{Ra} = \frac{\rho_{\mathrm{nf}}^2 \mathrm{g} \beta_{\mathrm{nf}} \Delta T H^3}{\mu_{\mathrm{nf}}^2} \mathrm{Pr_{nf}} \tag{20}$$

Numerical resolution and code validation

To numerically solve the PDE (1)-(7), we proceed to their discretizations in order to obtain a system of algebraic equations whose resolution allows us to determine the fields of all the variables of the problem considered. The finite volume method has been adopted to accomplish this discretization, and the developed SIMPLE algorithm for pressure correction.

The domain of computation is subdivided into finite number of elementary subdomains, called control volume. Each of these includes a node called the main node, as shown in fig. 2.

For a main node P, the points E and W (East and West) are neighbors in the direction *x-x*, the points N and S (North and South) are those in the direction *y-y*, while the points T and B (Bottom and Top) in the *z-z* direction. The control volume surrounding P is delimited by strong solid lines. The faces of the control volume are located at points e and w in the direction *x-x*, n and s in the direction *y-y* and t and b in the direction *z-z*.

Turbulent flows are significantly influenced near the walls. In fact, in the areas very close to the walls, the viscosity effects reduce the fluctuations in tangential speeds. Thus, to model the flows near the walls, we used a refined uniform mesh in the vicinity, fig. 3.

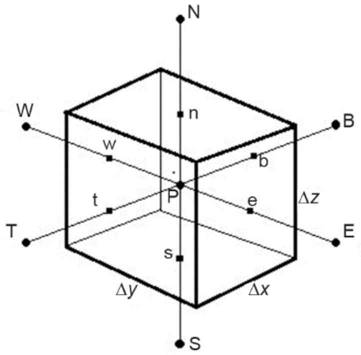

Figure 2. The 3-D control volume

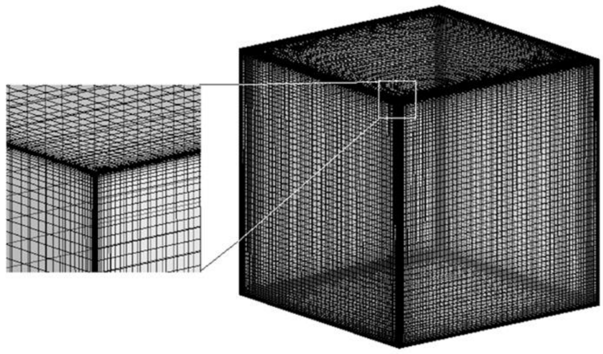

Figure 3. Refined uniform mesh near the walls

To study the influence of the mesh, we calculated the average Nu_{av} for different grids and for Rayleigh numbers 10^7, 10^8, and 10^9 to account for the turbulent regime. The results obtained for a cubic cavity filled with differentially heated water are presented in tab. 3.

Table 3. Validation of the grid for a cubic cavity

$Ra = 10^7$	Grid	40 × 40 × 40	60 × 60 × 60	80 × 80 × 80	100 × 100 × 100
	Nu_{av}	16.92200	17.13907	17.31362	17.35151
$Ra = 10^8$	Grid	40 × 40 × 40	60 × 60 × 60	80 × 80 × 80	100 × 100 × 100
	Nu_{av}	30.57809	31.24273	31.64807	31.75411
$Ra = 10^9$	Grid	40 × 40 × 40	60 × 60 × 60	80 × 80 × 80	100 × 100 × 100
	Nu_{av}	53.88716	55.99688	57.00166	57.30331

From tab. 3, it appears that the grid 80 × 80 × 80 is sufficiently fine to carry out the numerical simulations for the Rayleigh numbers 10^7, 10^8, and 10^9.

To discretize the governing equations, we are based on the finite volume method using the *power law* scheme which offers a good stability characteristic in the case of turbulent flows. The digital resolution of the problem was carried out by an elaborate FORTRAN code. The dynamic and thermal fields are calculated iteratively until the following convergence criterion is satisfied: the maximum residual value of mass, momentum, and thermal energy less than 10^{-6}.

To validate the numerical method, we compared the values of the Nu_{av} calculated on the cold wall of a cubic cavity filled with air with those found by Bilgen *et al.* [35], Dixit *et al.* [36], Bairi *et al.* [37], and Lankhorst [38]. The values of the mean Nusselt number calculated for the values of the Rayleigh number ($Ra = 10^7$ and $Ra = 10^8$) are presented in tab. 4.

Table 4. Comparison of average Nusselt number values with literature

Ra	Present	[35]	[36]	[37]	[38]
10^7	16.33	16.62	16.79	16.07	15.92
10^8	29.99	31.52	30.50	31.33	28.97

Table 4 shows a good agreement between the results of our code and those proposed by Bilgen *et al.* [35], Dixit *et al.* [36], Bairi *et al.* [37], and Lankhorst [38].

In fig. 4 we successively present the variations of the vertical speed 4(a) and the variations of the temperature 4(b) at mid-height in the median plane of the cavity.

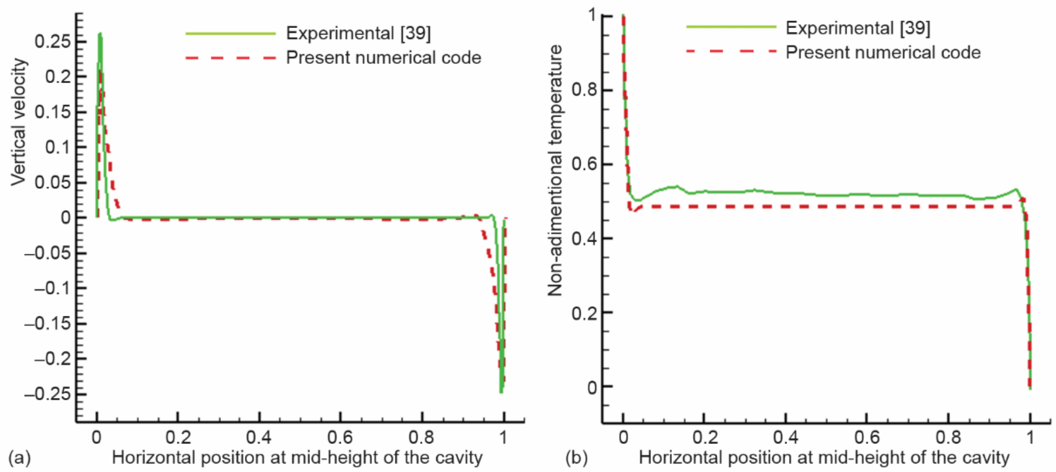

Figure 4. Variation of the vertical velocity (a) and the temperature (b) as a function of *X* at mid-height of the cavity

The values of speed are almost confused with those of experience. Furthermore, the temperature values show a good agreement with those of the experiment. The latter are slightly higher than those calculated numerically in the middle of the cavity.

Results and discussion

Figures 5 and 6 successively represent the temperature fields and the lines of currents inside a cubic cavity containing pure water in the two cases where the cavity is heated respectively by a vertical strip and another horizontal at the middle of one of the vertical walls.

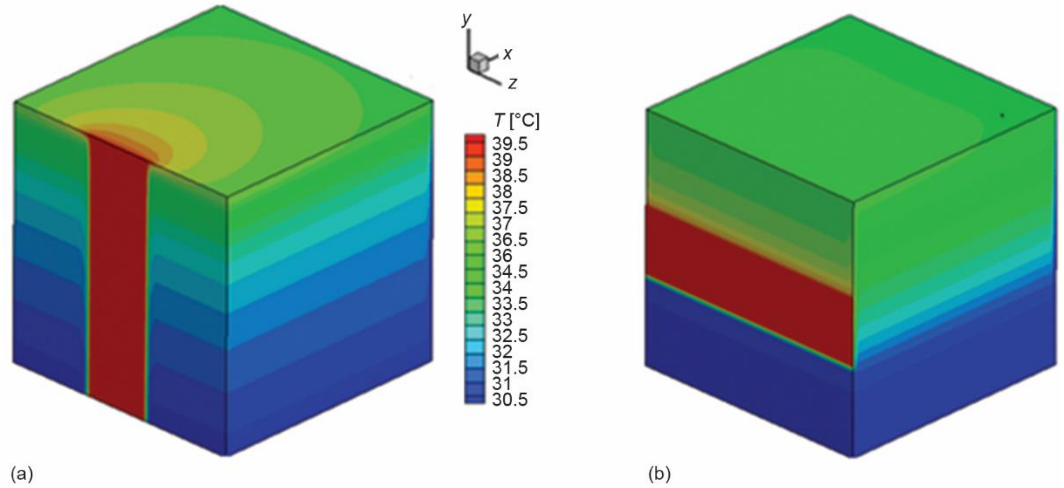

Figure 5. Isotherms contours of the pure water in a rectangular cavity for Ra = 10^9; (a) vertical configuration and (b) horizontal configuration

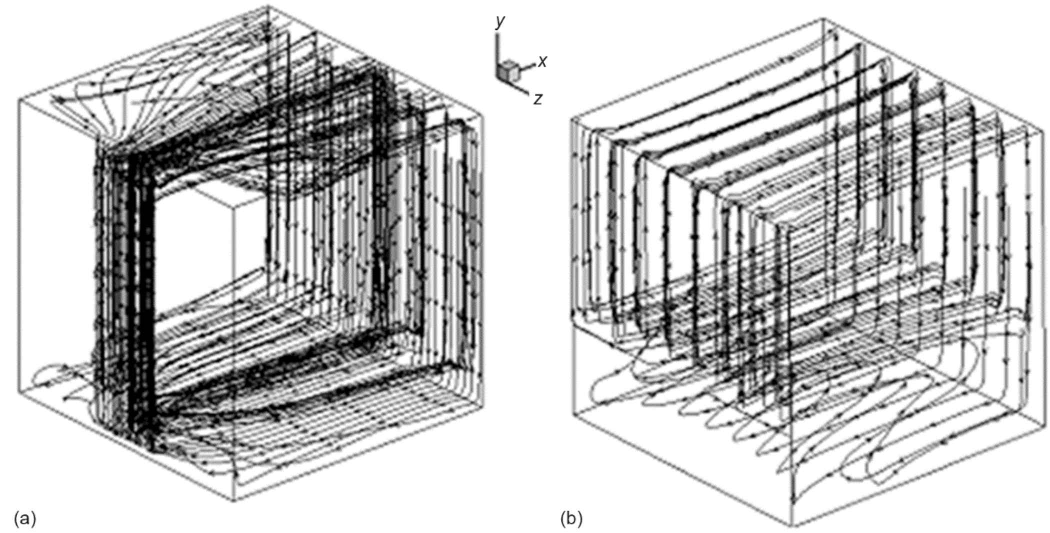

Figure 6. Streamlines of the pure water in a rectangular cavity for Ra = 10^9; (a) vertical configuration and (b) horizontal configuration

The isothermal lines and the current lines (for Ra = 10^9) represented successively by figs. 5 and 6 are marked by a stagnant horizontal stratification inside the cavity, which means that the heat transfer takes place for the most part by convection. It is also seen that the gradients of temperature and velocity become increasingly steep near the vertical walls, which shows that most of the turbulent flow occurs along the vertical sides of the cavity.

The Nu_{av} along the cold wall is shown in figs. 7-9 for different Rayleigh numbers (10^7, 10^8, and 10^9), for different types and volume fractions of nanoparticles (0-0, 02-0.04, and 0.06) in water and for both configurations (horizontal/vertical heating strip).

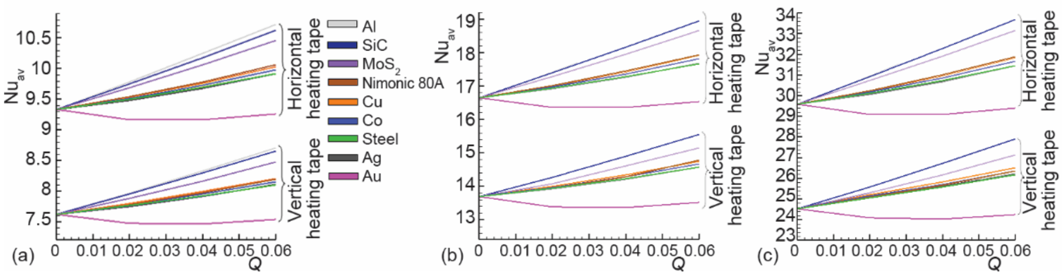

Figure 7. Variation of the mean Nusselt number as a function of the volume fractions of the metallic nanoparticles for Ra = 10^7 (a), Ra = 10^8 (b), and Ra = 10^9 (c)

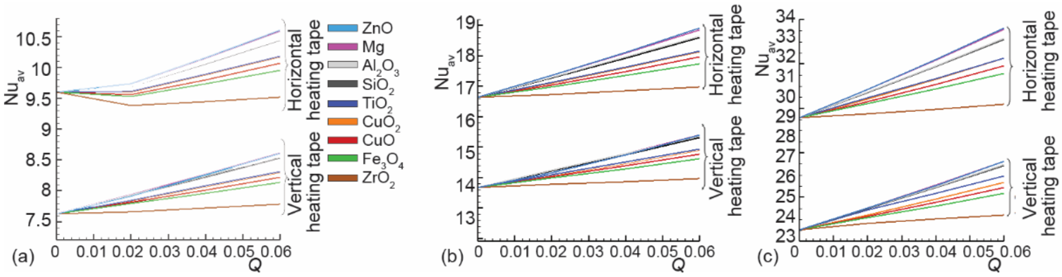

Figure 8. Variation of the mean Nusselt number as a function of the volume fractions of the metal oxide nanoparticles for Ra = 10^7 (a), Ra = 10^8 (b), and Ra = 10^9 (c)

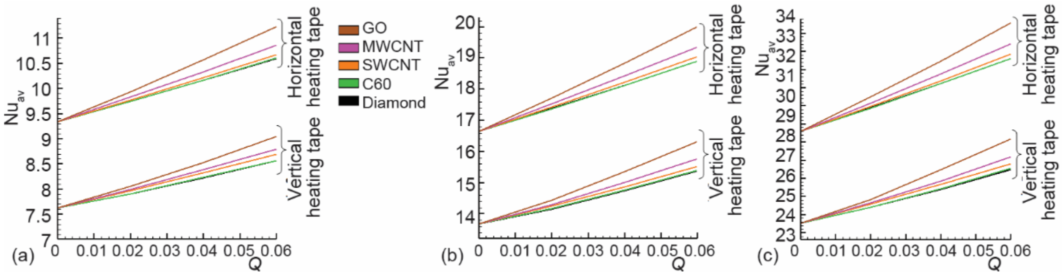

Figure 9. Variation in the mean Nusselt number as a function of the volume fractions of carbon-based nanoparticles for Ra = 10^7 (a), Ra = 10^8 (b), and Ra = 10^9 (c)

From the results, we can clearly see that the position of the heated partition considerably influences the heat exchange by natural convection. Indeed, figs. 7-9 show that the case where the heated partition is horizontal prevails and that the effect of this position is independent of the volume fraction of nanoparticles in water.

Figures 7-9 also show that the addition of the nanoparticles considerably improves the heat exchange by convection and that this improvement is all the greater as the number of Rayleigh is large. These figures represent an overview to compare the effect of the type of metal nanoparticles, metal oxide or carbon-based on turbulent natural convection.

We can also see that the carbon-based nanoparticles better intensify the heat exchange by convection and that their effect is even greater than the number of Rayleigh is large, in particular, for the grapheme oxide nanoparticles. This shows that grapheme oxide nanoparticles considerably improve the thermophysical properties of the fluid in turbulent flow. Thus, their use in suspension in heat transfer fluids can considerably improve the design of heat exchange systems in view of better optimization of space requirements.

On the other hand, figs. 7 and 8 also show that nanoparticles of gold and zirconium dioxide slow down heat transfer by convective flow. This shows that the addition of these nanoparticles in water deteriorates its thermo-physical properties in turbulent flow.

Conclusions

This work has studied numerically the effects of different nanoparticles (metallic, metallic oxide, and carbon-based) and the effect of the position of the heated partition on the heat transfer rate for turbulent natural convection at interior of a cubic cavity. Numerical simulations which are carried out for different Rayleigh numbers (10^7, 10^8, and 10^9) for different volume fractions of the nanoparticles and for the two positions of the heated partition (horizontal/vertical) have shown as follows.

- The horizontal position of the heated partition considerably improves the heat transfer by natural convection much better than the vertical position (there is an increase in the Nusselt number of more than 20%) and that the effect of this position is independent of the volume fraction of nanoparticles in water.
- The use of carbon-based nanoparticles suspended in water makes it possible to bring about a much greater improvement in thermal performance compared to the use of metallic nanoparticles or metallic oxide. This is due to their high thermal conductivities and their low densities.
- The effect of the type and volume fraction of nanoparticles on the value of the Nusselt number isis even greater than the number of Rayleigh is large.
- Unlike other nanoparticles, gold and zirconium dioxide nanoparticles deteriorate the thermo-physical properties of turbulent water, which slows thermal transfer by convective flow.

The results obtained clearly show that the use of nano-fluids based on carbon and in particular based on grapheme oxide and that the horizontal position of the heated partition can considerably influence the heat transfer by turbulent natural convection in this type of geometry.

Acknowledgment

I am grateful to all of those with whom I have had the pleasure to work during this and other related projects. Each of the members of my Dissertation Committee has provided me extensive personal and professional guidance and taught me a great deal about both scientific research and life in general. I would especially like to thank Dr. Sakina El Hamdani, the chairman of my committee. As my teacher and mentor, he has taught me more than I could ever give him credit for here.

I would like to thank my parents, whose love and guidance are with me in whatever I pursue. They are the ultimate role models. Most importantly, I wish to thank my loving and supportive wife, Naoual, and my son, Yahya, who provide unending inspiration.

Nomenclature

C_p – specific heat at constant pressure, [$\mathrm{Jkg^{-1}K^{-1}}$]
g – gravity acceleration, [$\mathrm{ms^{-2}}$]
G_k – buoyancy term
H – cavity height, [m]
k – turbulent kinetic energy, [$\mathrm{m^2s^{-2}}$]
K_{eff} – effective thermal conductivity
Nu – Nusselt number
p – pressure, [Pa]
P_k – stress production
Pr – Prandtl number

Ra – Rayleigh number
T – temperature, [K]
u, v, w – velocity components, [ms^{-1}]
x, y, z – cartesian co-ordinates, [m]

Greek symbols

a – thermal diffusivity, [m^{2}s^{-1}]
β – volumetric coefficient of thermal expansion, [K^{-1}]
ε – dissipation rate of turbulent kinetic energy
μ – dynamic viscosity, [Pa·s]
ρ – density, [kgm^{-3}]
σ_k, σ_t, σ_ε – numbers of turbulent Prandtl of k, t, and ε
Φ – particle volume fraction

Subscripts

av – average
c – cold
f – fluid
h – hot
nf – nanofluid
p – nanoparticle
ref – reference
t – turbulent

References

[1] Choi, S. U. S., Eastman, J. A., Enhancing Thermal Conductivity of fluIds with Nanoparticules, Developments and Applications of Non-Newtonian Flows, *American Society of Mechanical Engineers, 231* (1995), Nov., pp. 99-105
[2] Namburu, P. K., *et al.*, Numerical Study of Turbulent Flow and Heat Transfer Characteristics of Nanofluids Considering Variable Properties, *International Journal of Thermal Science, 48* (2009), 2, pp. 290-302
[3] Rabhi, R., *et al.*, Influence of Magnetohydrodynamic Viscous Flow on Entropy Generation Within Porous Micro Duct Using the Lattice Boltzmann Method, *RSC Advance, 7* (2017), 49, pp. 30673-30686
[4] Mirmasoumi, S., Bezadmehr, A., Effect of Nanoparticles Mean Diameter on Mixed Convection Heat Transfer of a Nanofluid in a Horizontal Tube, *International Journal of Heat and Fluid Flow, 29* (2008), 2, pp. 557-566
[5] Irfan, *et al.*, Heat Transfer in Natural Convection Flow of Nanofluid Along a Vertical Wavy Plate with Variable Heat Flux, *Thermal Science, 23* (2019), 1, pp. 179-190
[6] Fallah, *et al.*, Simulation of Natural Convection Heat Transfer Using Nanofluid in a Concentric Annulus, *Thermal Science, 21* (2017), 3, pp. 1275-1286
[7] Javed, S., *et al.*, Internal Convective Heat Transfer Ofnanofluids in Different Flow Regimes, A Comprehensive Review, *PHYSICA A: Statistical Mechanics and its Applications, 538* (2019), Jan., 122783
[8] Mendu, S., *et al.*, Simulation of Natural Convection of Nanofluidsin a Square Enclosure Embedded with Bottom Discrete Heater, *Thermal Science, 22* (2018), 6B, pp. 2771-2781
[9] Aghajani, D. M., *et al.*, Effect of Discrete Heater at the Vertical Wall of the Cavity Over the Heat Transfer and Entropy Generation Using Lattice Bolzmann Method, *Thermal Science, 15* (2011), 2, pp. 423-435
[10] Terekhov, V. I., *et al.*, Three-Dimensional Laminar Convection in a Parallelepiped with Heating of Two Side Walls, *Teplofizika Vysokikh Temperatur, 49* (2011), 6, pp. 905-911
[11] Mejia-Ariza, R., *et al.*, Formation of Hybrid Gold Nanoparticle Network Aggregates by Specific Host-Guest Interactions in a Turbulent Flow Reactor, *Journal of Materials Chemistry B, 2* (2014), 2, pp. 210-216
[12] Liu, Y., *et al.*, Turbulence in a Microscale Planar Confined Impinging-Jets Reactor, *Journal of Materials Chemistry B, 9* (2009), 8, pp. 1110-1118
[13] Sadiq, M. A., *et al.*, Numerical Simulation of Oscillatory Oblique Stagnation Point Flow of a Magneto Micropolar Nanofluid, *RSC Advance, 9* (2019), 9, pp. 4751-4764
[14] Peng, Y., *et al.*, A Numerical Simulation for Magnetohydrodynamic Nanofluid Flow and Heat Transfer in Rotating Horizontal Annulus with Thermal Radiation, *RSC Advance, 9* (2019), 39, pp. 22185-22197
[15] Sadeghi, G., *et al.*, Experimental and Numerical Investigations on Performance of Evacuated Tube Solar Collectors with Parabolic Concentrator, Applying Synthesized Cu_2O/Distilled Water Nanofluid, *Energy for Sustainable Development, 48* (2019), Feb., pp. 88-106
[16] Dogonchi, A. S., *et al.*, Heat Transfer by natural convection of Fe_3O_4-Water Nanofluid in an Annulus Between a Wavy Circular Cylinder and a Rhombus, *International Journal of Heat and Mass Transfer, 130* (2019), Mar., pp. 320-332

[17] Zaraki, A., *et al.*, Theoretical Analysis of Natural Convection Boundary Layer Heat and Mass Transfer of Nanofluids: Effects of Size, Shape and Type of Nanoparticles, Type of base Fluid and Working Temperature, *Advanced Powder Technology, 26* (2015), 3, pp. 935-946
[18] Jahanshahi, M., *et al.*, Numerical Simulation of Free Convection Based on Experimental Measured Conductivity in a Square Cavity usIng Water/SiO_2 Nanofluid , *International Communications in Heat and Mass Transfer, 37 (*2010), 6, pp. 687-694
[19] Zangooee, M. R., *et al.*, Hydrothermal Analysis of MHD Nanofluid (TiO_2-GO) flow Between Two Radiative Stretchable Rotating Disks Using AGM, *Case Studies in Thermal Engineering, 14* (2019), Sept., 100460
[20] Haddad, O., *et al.*, Free Convection in ZnO-Water Nanofluid-Filled and Tilted Hemispherical Enclosures Containing a Cubic Electronic Device, *International Communications in Heat and Mass Transfer, 87* (2017), Oct., pp. 204-211
[21] Iqbal, S. M., *et al.*, A Comparative Investigation of AL_2O_3/H_2O, SIO_2/H_2O and ZRO_2/H_2O Nanofluid for Heat Transfer Applications, *Digest Journal of Nanomaterials and Biostructures, 12* (2017), 2, pp 255-263
[22] Aman, S., *et al.*, Impacts of Gold Nanoparticles on MHD Mixed Convection Poiseuille Flow of Nanofluid Passing Through a Porous Mediumin the Presence of Thermal Radiation, *Thermal Diffusion and Chemical Reaction. Neural Comput. & Applic., 30* (2018), 3, pp. 789-797
[23] Kefayati, G. H. R., Simulation of Ferrofluid Heat Dissipation Effect on Natural Convection at an Inclined Cavity Filled with Kerosene/Cobalt Utilizing the Lattice Boltzmann Method, *Numerical Heat Transfer, Part A: Applications, 65* (2014), 6, pp. 509-530
[24] Shafie, Sh., *et al.*, Molybdenum Disulfide Nanoparticles Suspended in Water-Based Nanofluids with Mixed Convection and Flow inside a Channel filled with Saturated Porous Medium, *AIP Conference Proceedings, 1775* (2016), 1, 030042
[25] Sandeep, N., *et al.*, Effects of Radiation on an Unsteady Natural Convective Flow of a EG-Nimonic 80a Nanofluid Past an Infinite Vertical Plate, *Advances in Physics Theories and Applications, 23* (2013), May, pp. 36-43
[26] Benabderrahmane, A., Numerical Study of the Application of Nanofluids in Improving Heat Transfer in Solar Sensors, Ph. D. thesis, (in French), Djillali Liabes University, Sidi Bel Abbès, Algérie, 2017
[27] Salman, S. D., *et al.*, Numerical Investigation of Heat Transfer and Friction Factor Characteristics in a Circular Tube Fitted with V-Cut Twisted Tape Inserts, *The Scientific World Journal, 2013* (2013), ID792762
[28] Gunnasegaran, P., *et al.*, Numerical Study of Fluid Dynamic and Heat Transfer in a Compact Heat Exchanger Using Nanofluids, *International Scholarly Research Network ISRN Mechanical Engineering*, *2012* (2012), ID585496
[29] Selimefendigil, F., *et al.*, Mixed convection in a lid-driven cavity filled with single and multiple walled carbon nanotubes nanofluid having an inner elliptic obstacle, *Propulsion and Power Research*, *8* (2018), 2, pp. 128-137
[30] Brinkman, H. C., The Viscosity of Concentrated Suspensions and Solutions, *Journal of Chemical Physics, 20* (1952), 4, pp. 571-581
[31] Maxwell, J. C., *A Treatise on Electricity and Magnetism*, Clarendon Press, Wotton-under-Edge, UK, 1891
[32] Pak, B. C., *et al.*, Hydrodynamic and Heat Transfer Study of Dispersed Fluids with Submicron Metallic Oxide Particles, *Experimental Heat Transfer, 11* (1998), 2, pp. 151-170
[33] Launder, B. E., Spalding, D. B., The Numerical Computation of Turbulent Flows, *Computer Methods in Applied Mechanics and Engineering*, *3* (1974), 2, pp 269–289
[34] Henkes, *et al.*, Comparison of the Standard Case for Turbulent Natural Convection in a Square Enclosure, In a Seminar on Turbulent Natural Convection in Enclosures: A Computational and Experimental Benchmark Study, *Proceedings (R. A. W. M. Henkes and C. J. Hoogendoorn)*, Delft, Netherlands, 1992, 22, pp. 185-213
[35] Bilgen, E., *et al.*, Naturel Convection in Cavities with a Thin Fin on the Hot Wall, *International Journal of Heat and Mass Transfer, 48* (2005), 17, pp. 3493-3505
[36] Dixit, *et al.*, Simulation of High Rayleigh Number Convection in a Square Cavity Using the Lattice Boltzmann Method, *International Journal of Heat and Mass Transfer, 49* (2006), 3-4, pp. 727-739

[37] Bairi, A., *et al.*, Nusselt-Rayleigh Correlations for Design of Industrial Elements Experimental and Numerical Investigation of Natural Convection in Tilted Square Air Filled Enclosures, *Energy Conversion and Management, 49* (2008), 4, pp. 771-782
[38] Lankhorst, A. M., Laminar and Turbulent Natural Convection in Cavities – Numerical Modelling and Experimental Validation, Ph. D. thesis, Technology University of Delft, Delft, The Netherlands, 1991
[39] Ampofo, *et al.*, Experimental Benchmark Data for Turbulent Natural Convection in an Air Filled Square Cavity, *International Journal of Heat and Mass Transfer, 46* (2003), 19, pp. 3551-3572

Paper submitted: May 13, 2020
Paper revised: September 9, 2020
Paper accepted: October 10, 2020